Research Square

Preprints are preliminary reports that have not undergone peer review.
They should not be considered conclusive, used to inform clinical practice,
or referenced by the media as validated information.

Long-term mortality, refracture, and 1-year mortality risk after osteoporotic fracture: development in a public cohort and external validation in an independent hospital cohort

Jintao Xi
Wuhan Integrated Traditional Chinese and Western Medicine Orthopedic Hospital, Affiliated Hospital of Wuhan Sports University

Tao Li
Wuhan Integrated Traditional Chinese and Western Medicine Orthopedic Hospital, Affiliated Hospital of Wuhan Sports University

Biwang Huang
General Hospital of Central Theater Command of the Chinese People's Liberation Army

Jun Ma
General Hospital of Central Theater Command of the Chinese People's Liberation Army

Chengjie Xiong
General Hospital of Central Theater Command of the Chinese People's Liberation Army

Feng Xu
General Hospital of Central Theater Command of the Chinese People's Liberation Army

Qilin Lu
Wuhan Integrated Traditional Chinese and Western Medicine Orthopedic Hospital, Affiliated Hospital of Wuhan Sports University

Hang He
gkhh0418@gmail.com

General Hospital of Central Theater Command of the Chinese People's Liberation Army

Research Article

Keywords:

Posted Date: November 1st, 2026

DOI: https://doi.org/10.21203/rs.3.rs-11192346/v1

License: This work is licensed under a Creative Commons Attribution 4.0 International License.
Read Full License

Additional Declarations: No competing interests reported.

Abstract

Background

Long-term mortality and refracture are major outcomes after osteoporotic fracture, yet their prognostic patterns may differ according to fracture category and patient characteristics. We aimed to characterize long-term mortality, refracture risk, and post-fracture pathways after osteoporotic fracture and to develop and externally validate a parsimonious model for 1-year post-discharge mortality.

Methods

We conducted a retrospective prognostic study using a publicly available development cohort and an independent hospital-based external validation cohort. The development cohort comprised 4,773 patients with osteoporotic fractures reconstructed from a publicly released longitudinal dataset. Long-term all-cause mortality was estimated from index admission using Kaplan–Meier methods, whereas first refracture was analysed using cumulative incidence functions with death treated as a competing event. Adjusted prognostic associations were assessed using Cox, cause-specific Cox, and Fine–Gray models, and post-fracture transitions were summarized descriptively. A nine-variable Cox proportional hazards model incorporating age, sex, fracture category, body mass index, ASA class, source-provided Charlson Comorbidity Index, haemoglobin, albumin, and creatinine was developed to estimate 365-day mortality after discharge. Internal validation used 500 patient-level bootstrap samples, with multiple imputation re-estimated within each resample. The frozen model was then applied without refitting to an independent retrospective hospital cohort of 695 patients, among whom 28 deaths occurred within 365 days.

Results

In the development cohort, 5-year all-cause mortality was 17.64% (95% CI, 16.19–19.22), compared with a 5-year cumulative incidence of first refracture of 8.41% (95% CI, 7.30–9.51). Mortality was highest after hip/femur fracture, reaching 32.10% at 5 years (95% CI, 29.24–35.17). Female sex was associated with lower mortality (HR, 0.64; 95% CI, 0.54–0.76) but higher refracture risk (cause-specific HR, 1.47; 95% CI, 1.09–1.98; Fine–Gray sHR, 1.54; 95% CI, 1.14–2.08). Lumbar spine/pelvis and thoracic spine/rib fractures were similarly associated with lower mortality than hip/femur fracture but higher refracture risk. After optimism correction, the 365-day IPCW time-dependent AUC in the development cohort was 0.860, with a calibration slope of 0.958. In the external cohort, the AUC for 365-day mortality was 0.802 (95% CI, 0.709–0.884), the calibration slope was 0.849 (95% CI, 0.540–1.237), and the observed-to-expected ratio was 1.006 (95% CI, 0.667–1.387). Twenty of the 28 deaths (71.4%) occurred in the highest predicted-risk quintile. Findings were materially unchanged in the outcome-informed multiple-imputation sensitivity analysis.

Conclusions

Patients hospitalized with osteoporotic fractures experienced substantial long-term mortality and refracture burden, with distinct prognostic patterns across fracture categories and patient characteristics. A parsimonious clinical Cox model retained good discrimination and close overall calibration for 1-year post-discharge mortality when applied without refitting to an independent hospital cohort. The model may provide a practical basis for post-fracture mortality risk stratification and warrants further evaluation across broader clinical settings.

Introduction

Osteoporotic fractures are a major cause of morbidity, loss of independence, and premature death in older adults. Excess mortality has been documented not only after hip fracture but also after other major osteoporotic fractures, with both the magnitude and duration of risk varying by fracture site and patient characteristics [1–3]. Hip fracture is associated with particularly high early and long-term mortality, whereas vertebral and other non-hip fractures also contribute substantially to subsequent mortality and functional decline [4–7]. With population ageing, the global burden of fragility fractures and their long-term consequences is expected to rise further [8–10]. Most previous studies, however, have focused on individual fracture sites or have examined mortality and refracture separately, limiting an integrated understanding of prognosis across osteoporotic-fracture populations.

Refracture is another major component of post-fracture morbidity. A previous fragility fracture substantially increases the risk of a subsequent fracture, particularly soon after the index event [11–15]. In older patients, this risk occurs alongside substantial competing mortality, especially after hip or femoral fracture, where death may occur before a subsequent fracture is observed [16–18]. Competing-risk methods are therefore important for estimating the absolute probability of refracture in these populations. Mortality and refracture may also follow distinct prognostic patterns, with age, sex, fracture site, and comorbidity contributing differently to each outcome [2, 3, 18, 19]. Evaluating both outcomes within a common analytical framework may therefore provide a more complete picture of post-fracture prognosis.

These differences are also relevant to post-discharge risk stratification. Most established mortality prediction tools were developed in patients undergoing surgery for hip fracture and primarily target short-term postoperative mortality [20, 21]. More recent studies have extended prediction to broader fracture populations, but independent external validation and detailed assessment of calibration remain less common [22]. Reliable risk stratification therefore requires assessment of both discrimination and calibration in an independent setting [23, 24]. We aimed to (1) quantify long-term all-cause mortality and first-refracture risk after osteoporotic fracture while accounting for competing mortality; (2) examine adjusted prognostic associations and describe post-fracture transition patterns; and (3) develop and internally validate a parsimonious clinical model for 1-year post-discharge mortality and evaluate its performance in an independent external cohort.

Methods

Study design, data sources, and participants

We conducted a retrospective prognostic cohort study using two independent data sources. Model development and internal validation were based on a publicly available longitudinal dataset, whereas external validation was performed in an independent retrospective hospital cohort.

Development cohort

Development data were obtained from the publicly available Osteoporotic Fracture Registration System (OPFRS) dataset established at the Affiliated Kunshan Hospital of Jiangsu University, Jiangsu Province, China. The source registry included adults aged 50 years or older who were hospitalized with osteoporotic fractures and linked clinical records to the Kunshan Regional Health Registration Platform and the Jiangsu Provincial Population Death Registration System using encrypted patient identifiers [25]. The publicly released dataset contained 4,782 registered patients.

For the present secondary analysis, six records with irreconcilable date conflicts and three with inconsistent total-cost information were excluded, leaving 4,773 patients in the development cohort. This cohort was reconstructed from the complete publicly released dataset and therefore differed from the 4,325-patient analytical cohort reported in the original data publication, which applied additional eligibility criteria for its own study objectives [25].

In the source registry, osteoporotic fractures were operationally identified in adults aged ≥ 50 years with low-trauma fractures involving predefined skeletal sites [25]. For the present study, index fractures were classified into five categories: hip/femur, lumbar spine/pelvis, thoracic spine/rib, forearm/wrist, and shoulder/proximal humerus.

External validation cohort

An independent retrospective external validation cohort was assembled from patients hospitalized in the Department of Orthopaedics, Wuhan Integrated Traditional Chinese and Western Medicine Orthopedic Hospital/Affiliated Hospital of Wuhan Sports University, Wuhan, China, between June 1, 2023 and June 1, 2025.

Eligibility for the external cohort was based on an operational definition of osteoporotic or fragility fracture used for this retrospective study. Patients were eligible if they had either a documented diagnosis of osteoporosis, including a DXA T-score ≤ − 2.5 at the lumbar spine, femoral neck, or total hip, or a clinically documented low-energy fragility fracture involving one of the predefined fracture sites [26].

Patients were included if they met all of the following criteria: (1) age ≥ 50 years at the index hospitalization; (2) hospitalization for an osteoporotic or fragility fracture classifiable into one of the five fracture categories used in the development cohort; (3) fulfillment of the operational osteoporosis or fragility-fracture definition described above; and (4) availability of all predictors required by the frozen prediction model and ascertainment of 365-day post-discharge mortality status.

Patients were excluded for high-energy trauma or malignancy-related pathological fracture; a fracture that could not be assigned to one of the five predefined categories; unresolved inconsistencies in key dates or other critical clinical information that prevented reliable determination of follow-up or model predictors; or missing frozen-model predictors or incomplete ascertainment of 365-day post-discharge mortality.

Vital status through 365 days after discharge was ascertained from hospital electronic records and structured follow-up records, supplemented by telephone follow-up when required. For patients with more than one eligible hospitalization during the study period, only the first qualifying admission was retained as the index hospitalization. The final external validation cohort comprised 695 patients, of whom 28 died within 365 days after discharge. The patient-selection process is shown in Supplementary Fig. S1.

The source registry study was approved by the Institutional Review Board of the Affiliated Kunshan Hospital of Jiangsu University (approval No. 2024-03-053-H00-K01), with the requirement for informed consent waived because of the retrospective design and use of de-identified data [25]. The independent external validation study was approved by the Ethics Committee of Wuhan Integrated Traditional Chinese and Western Medicine Orthopedic Hospital/Affiliated Hospital of Wuhan Sports University (approval No. 672HREC20260522-L044), which waived the requirement for individual informed consent because of the retrospective use of routinely collected clinical data. Both study components were conducted in accordance with the Declaration of Helsinki.

Outcomes and analytical time scales

Three analytical time scales were defined according to the study question.

For mortality analyses, time zero was the index hospital admission. In the publicly released dataset, April 24, 2024 was uniformly recorded in the death-time field for patients coded as alive, whereas observed dates of death were recorded for patients who died. The latest recorded death occurred on April 20, 2024. April 24, 2024 was therefore used as the administrative endpoint for mortality ascertainment. Cumulative all-cause mortality was estimated at 30 days and at 1, 3, and 5 years.

For first-refracture and post-fracture transition analyses, time zero was also the index admission. March 24, 2024 was uniformly recorded for patients without a documented first refracture in the released dataset and was therefore used as the common administrative cutoff for analyses involving both refracture and death. Death before first refracture was treated as a competing event [27, 28]. Deaths

occurring after March 24 and on or before April 24, 2024 contributed to the mortality analyses but were censored on March 24, 2024 in the competing-risk and transition analyses.

For prediction modelling, time zero was hospital discharge and the target outcome was all-cause mortality within 365 days after discharge. Patients who remained alive but had less than 365 days of available follow-up were censored at their last observed follow-up. Seven patients died on the day of discharge; their event time was set to 0.5 days to retain these events in the Cox analysis while ensuring a positive event interval.

Baseline variables

Baseline variables included age, sex, index-fracture category, body mass index (BMI), American Society of Anesthesiologists (ASA) physical-status class, source-provided Charlson Comorbidity Index (CCI), haemoglobin, serum albumin, serum creatinine, and admission year.

The source-provided CCI was used as recorded in the publicly released dataset and did not include age points. ASA class was dichotomized as III–IV versus I–II in the prognostic and prediction models. Creatinine was log2-transformed so that the corresponding regression coefficient represented the association with a doubling in serum creatinine.

Age was modelled nonlinearly in the mortality and prediction models using restricted cubic splines with knots at 54, 68, and 85 years [29].

Because the public data dictionary did not specify the exact timing of haemoglobin, albumin, creatinine, ASA classification, or CCI assessment during the index hospitalization, these variables were treated as clinical information recorded during hospitalization and available by discharge.

Long-term mortality analysis

Cumulative all-cause mortality was estimated from index admission through April 24, 2024 using the Kaplan–Meier method. Estimates with 95% confidence intervals and numbers at risk were reported at the specified time points. Follow-up duration was estimated using the reverse Kaplan–Meier method.

Adjusted associations with long-term mortality were estimated using multivariable Cox proportional hazards regression. The model included age, sex, fracture category, BMI, ASA class, source-provided CCI, haemoglobin, albumin, log2-transformed creatinine, and admission year.

Age was represented using restricted cubic splines and interpreted jointly rather than as a single per-year hazard ratio. The overall association between age and mortality and evidence of departure from linearity were assessed using joint Wald tests of the spline coefficients. The proportional hazards assumption was assessed using scaled Schoenfeld residuals across the imputed datasets [30].

Refracture and competing-risk analyses

The cumulative incidence of first refracture was estimated through March 24, 2024, with death before first refracture treated as a competing event. Differences across the five fracture categories were assessed using Gray's test [31].

Associations with first refracture were evaluated using cause-specific Cox and Fine–Gray regression. Cause-specific Cox regression estimated associations with the instantaneous refracture hazard among patients who remained alive and refracture-free, whereas Fine–Gray regression estimated subdistribution hazard ratios for the cumulative incidence of refracture in the presence of competing mortality [27, 28].

Both models included the same adjustment variables. Age was expressed per 10-year increase in the refracture analyses. Cause-specific and subdistribution hazard ratios were interpreted as distinct estimands [28].

Descriptive post-fracture disease transitions

Post-fracture trajectories were summarized using a three-state framework comprising survival without refracture, first refracture, and death. These analyses used the same administrative cutoff of March 24, 2024 as the competing-risk analyses.

Three observed transitions were evaluated: survival without refracture to first refracture, survival without refracture to direct death, and first refracture to death. For each transition, we calculated the number of events, accumulated person-time, and crude transition rate per 1,000 person-years with 95% confidence intervals.

These analyses were descriptive and were used to characterize observed post-fracture pathways.

Development of the 1-year mortality prediction model

A multivariable Cox proportional hazards model was developed to estimate individual risk of all-cause mortality within 365 days after hospital discharge.

The model contained nine routinely available clinical inputs: age, sex, fracture category, BMI, ASA class, source-provided CCI, haemoglobin, albumin, and creatinine. Age was represented using restricted cubic splines with knots at 54, 68, and 85 years, and creatinine was log2-transformed. Hip/femur fracture served as the reference category.

The predictor set, functional forms, and model class were defined before final model fitting. No repeated predictor selection, automated stepwise selection, or comparison across multiple machine-learning algorithms was undertaken in the final model-development procedure. Bootstrap-based internal

validation was used instead of random sample splitting to preserve the full development sample and quantify optimism [32].

Individual 365-day mortality risk was calculated from the Cox linear predictor and the frozen baseline survival function.

Missing data and multiple imputation

Four predictors contained missing values in the development cohort: BMI in 755 patients (15.8%), haemoglobin in 91 (1.9%), albumin in 155 (3.2%), and creatinine in 59 (1.2%).

Missing baseline covariates were handled using multiple imputation by chained equations. The primary imputation model included 17 baseline variables: the nine prediction-model inputs together with admission year, hypertension, diabetes, heart disease, cerebrovascular disease, chronic kidney disease, surgery, and anti-osteoporosis treatment.

Predictive mean matching was used to impute BMI, haemoglobin, albumin, and creatinine [33]. The remaining variables in the primary imputation model were completely observed. Thirty imputed datasets were generated for the principal prognostic analyses, and adjusted estimates were combined using Rubin's rules.

The primary imputation model did not include outcome or follow-up information. An outcome-informed multiple-imputation sensitivity analysis was additionally performed by incorporating event status and cumulative-hazard information [34].

Internal validation

Internal validation of the prediction model was performed using 500 patient-level bootstrap samples [32].

Within each bootstrap repetition, the multiple-imputation model was re-estimated in the resampled dataset and five imputed datasets were generated. The Cox model was then refitted in the bootstrap sample and evaluated in both the bootstrap sample and the original development dataset.

For each performance measure, optimism was calculated as the difference between performance in the bootstrap sample and performance when the fitted model was applied to the original development dataset. Mean optimism across the 500 repetitions was subtracted from the corresponding full-data apparent estimate to obtain optimism-corrected performance.

Because 355 patients were censored alive before 365 days, discrimination at 365 days was assessed using an inverse-probability-of-censoring-weighted time-dependent AUC. Harrell's C statistic was used to assess overall rank discrimination while accounting for censoring, and prediction error at 365 days was assessed using a censoring-adjusted Brier score.

Calibration was evaluated using calibration-in-the-large, calibration slope, mean predicted risk, observed risk, and the observed-to-expected (O/E) event ratio. The integrated Brier score was additionally calculated as a summary measure of prediction error over time [23].

Replicate-specific corrected distributions represented variation in estimated optimism rather than full sampling uncertainty. Internal performance was therefore summarized using optimism-corrected point estimates.

A secondary sensitivity analysis used 100 bootstrap repetitions with 10 imputations per repetition.

Outcome-informed multiple-imputation sensitivity analysis

An additional sensitivity analysis examined the effect of incorporating outcome information into the imputation model.

The sensitivity imputation model retained the same 17 baseline variables and additionally included the 365-day mortality indicator and standardized Nelson–Aalen cumulative hazard as auxiliary variables [34]. Thirty imputed datasets were generated.

The predictor set, variable definitions, transformations, restricted cubic-spline knots, and model structure remained unchanged. Model stability was assessed by comparing regression coefficients, linear predictors in the development and external cohorts, individual predicted risks, AUC, Harrell's C statistic, Brier score, calibration slope, and O/E ratio. Results were materially unchanged, and the frozen prediction model was retained without refitting.

External validation

The complete prediction model was frozen before external validation and applied without refitting to the independent external cohort of 695 patients.

All external-validation patients had complete predictor data and complete ascertainment of 365-day post-discharge vital status. The AUC for 365-day mortality was therefore calculated from the complete binary 365-day outcome rather than using a censoring-weighted time-dependent ROC method. Harrell's C statistic was additionally calculated from the survival data, and overall predictive accuracy was evaluated using the 365-day Brier score.

Calibration was assessed using calibration-in-the-large, calibration slope, and the O/E event ratio [23]. External performance measures were reported with 95% confidence intervals. Calibration was also assessed graphically across quintiles of predicted risk by comparing observed mortality with mean predicted risk within each group.

Transportability was examined by comparing individual predictor distributions and the model linear predictor between the development and external cohorts. Standardized mean differences quantified

differences in predictor distributions between cohorts, and the ratio of external to development linear-predictor standard deviations characterized differences in overall risk dispersion.

Risk stratification and model updating

For descriptive risk stratification, patients in the external cohort were divided into quintiles according to predicted 365-day mortality risk. Observed mortality and mean predicted risk were summarized within each quintile, and the proportion of all external deaths occurring in the highest predicted-risk quintile was calculated.

The quintiles were used to describe the concentration of predicted risk rather than to define intervention thresholds.

Two secondary recalibration strategies were explored after evaluation of the unchanged frozen model. The first updated calibration-in-the-large while fixing the calibration slope at 1. The second estimated both calibration-in-the-large and the calibration slope. Updated models were compared with the unchanged frozen model using discrimination, calibration, and Brier score. The frozen model remained the primary external-validation model.

Decision-curve analysis

Decision-curve analysis was used to explore the net benefit of the frozen model across a range of risk thresholds compared with treat-all and treat-none strategies [24]. Uncertainty was quantified using 2,000 patient-level bootstrap samples.

Statistical analysis and reporting

Continuous variables were summarized as mean (standard deviation) or median [interquartile range], as appropriate, and categorical variables as number (percentage). Differences in baseline characteristics between the development and external validation cohorts were quantified using standardized mean differences.

Effect estimates, absolute-risk estimates, and external-validation performance measures are presented with 95% confidence intervals where applicable. All statistical tests were two-sided.

Analyses were performed using R version 4.5.2 (R Foundation for Statistical Computing, Vienna, Austria), principally with the survival, mice, cmprsk, Hmisc, and pROC packages. ggplot2 was used for graphical presentation.

The observational components of the study were reported in accordance with the Strengthening the Reporting of Observational Studies in Epidemiology (STROBE) statement [35], and the prediction-model development and external-validation components were reported according to the TRIPOD + AI reporting guideline [36].

Results

Study population and analytical cohorts

Of 4,782 patients in the publicly released source dataset, six were excluded because of irreconcilable date inconsistencies and three because of inconsistent total-cost information, leaving 4,773 patients in the development cohort (Fig. 1A). The mean age was 68.8 years (SD 11.2), and 3,230 patients (67.7%) were women. Index fractures involved the hip/femur in 1,686 patients (35.3%), lumbar spine/pelvis in 1,289 (27.0%), thoracic spine/rib in 722 (15.1%), forearm/wrist in 667 (14.0%), and shoulder/proximal humerus in 409 (8.6%) (Table 1).

Table 1
Baseline characteristics of the development and external validation cohorts

Characteristic	Summary	Development cohort (n = 4,773)	External validation cohort (n = 695)	Development cohort missing, n (%)	Absolute SMD
Patients	n	4,773	695	—	—
Age (years)	Mean (SD)	68.8 (11.2)	69.3 (10.6)	0 (0.0%)	0.054
Female	n (%)	3,230 (67.7%)	470 (67.6%)	0 (0.0%)	0.001
Hip/femur	n (%)	1,686 (35.3%)	246 (35.4%)	0 (0.0%)	0.002
Lumbar spine/pelvis	n (%)	1,289 (27.0%)	196 (28.2%)	0 (0.0%)	0.027
Thoracic spine/rib	n (%)	722 (15.1%)	112 (16.1%)	0 (0.0%)	0.027
Forearm/wrist	n (%)	667 (14.0%)	91 (13.1%)	0 (0.0%)	0.026
Shoulder/proximal humerus	n (%)	409 (8.6%)	50 (7.2%)	0 (0.0%)	0.051
BMI (kg/m²)	Mean (SD)	23.3 (3.3)	23.2 (3.3)	755 (15.8%)	0.017
ASA I	n (%)	590 (12.4%)	86 (12.4%)	0 (0.0%)	0.000
ASA II	n (%)	3,116 (65.3%)	453 (65.2%)	0 (0.0%)	0.002
ASA III	n (%)	1,049 (22.0%)	153 (22.0%)	0 (0.0%)	0.001
ASA IV	n (%)	18 (0.4%)	3 (0.4%)	0 (0.0%)	0.009
Source-provided CCI	Median [Q1, Q3]	0.0 [0.0, 0.0]	0.0 [0.0, 0.0]	0 (0.0%)	0.170
Haemoglobin (g/L)	Mean (SD)	125.1 (18.3)	124.1 (17.9)	91 (1.9%)	0.054
Albumin (g/L)	Mean (SD)	39.9 (4.4)	40.0 (4.1)	155 (3.2%)	0.001

Values and continuous-variable SMDs use available, nonmissing observations before development-cohort imputation.

There were no missing predictor values in the external validation cohort.

Absolute SMDs use the pooled within-cohort standard deviation; categorical level rows use binary contrasts.

Global fracture-type SMD: 0.064; model ASA III-IV vs I-II SMD: 0.002. These complete-data contrasts match the transportability audit.

Characteristic	Summary	Development cohort (n = 4,773)	External validation cohort (n = 695)	Development cohort missing, n (%)	Absolute SMD
Creatinine (μmol/L)	Median [Q1, Q3]	61.0 [51.0, 74.0]	63.4 [45.9, 86.7]	59 (1.2%)	0.114
Values and continuous-variable SMDs use available, nonmissing observations before development-cohort imputation.					
There were no missing predictor values in the external validation cohort.					
Absolute SMDs use the pooled within-cohort standard deviation; categorical level rows use binary contrasts.					
Global fracture-type SMD: 0.064; model ASA III-IV vs I-II SMD: 0.002. These complete-data contrasts match the transportability audit.					

The independent retrospective external validation cohort comprised 695 patients treated between June 1, 2023 and June 1, 2025, among whom 28 deaths occurred within 365 days after discharge. The patient-selection process is shown in Supplementary Fig. S1. All predictors required by the frozen model and 365-day mortality status were complete in the external cohort. Baseline characteristics were generally similar between cohorts. The largest absolute standardized mean differences among individual predictors were observed for the source-provided CCI (0.170) and creatinine (0.114), whereas the global standardized mean difference was 0.064 for fracture category and 0.002 for ASA III–IV versus I–II (Table 1; Table S7).

The 4,773 patients in the development cohort contributed to three parallel analytical components with outcome-specific time scales (Fig. 1C). Long-term mortality was assessed from index admission through April 24, 2024. Refracture and descriptive state-transition analyses used index admission as time zero and March 24, 2024 as the common administrative cutoff. The prediction model targeted all-cause mortality within 365 days after hospital discharge. Within the development cohort, 201 deaths occurred within 365 days, while 355 patients remained alive but were censored before 365 days because of shorter available follow-up.

Long-term mortality and refracture burden

During long-term follow-up, 574 deaths occurred in the development cohort. Cumulative all-cause mortality was 0.44% (95% CI, 0.29–0.67) at 30 days, 4.08% (95% CI, 3.55–4.68) at 1 year, 10.47% (95% CI, 9.53–11.50) at 3 years, and 17.64% (95% CI, 16.19–19.22) at 5 years (Fig. 2A; Table 2).

Table 2
Absolute risks after osteoporotic fracture

Outcome	30 days	1 year	3 years	5 years
All-cause mortality	0.44 (0.29–0.67)%	4.08 (3.55–4.68)%	10.47 (9.53–11.50)%	17.64 (16.19–19.22)%
First refracture (competing-risk CIF)	—	1.67 (1.30–2.04)%	4.76 (4.07–5.45)%	8.41 (7.30–9.51)%
5-year mortality by index fracture category	—	—	—	—
Hip/femur	—	—	—	32.10 (29.24–35.17)%
Lumbar spine/pelvis	—	—	—	11.03 (8.85–13.71)%
Thoracic spine/rib	—	—	—	10.97 (8.12–14.75)%
Forearm/wrist	—	—	—	3.36 (1.85–6.07)%
Shoulder/proximal humerus	—	—	—	5.99 (2.78–12.68)%

Values are cumulative risk estimates (95% CI). Mortality uses Kaplan-Meier estimation; first refracture uses a cumulative incidence function with death as a competing event.

Mortality varied across fracture categories (Fig. 2B; Supplementary Fig. S3). Five-year mortality was highest after hip/femur fracture, at 32.10% (95% CI, 29.24–35.17). Corresponding estimates were 11.03% (95% CI, 8.85–13.71) after lumbar spine/pelvis fracture, 10.97% (95% CI, 8.12–14.75) after thoracic spine/rib fracture, 3.36% (95% CI, 1.85–6.07) after forearm/wrist fracture, and 5.99% (95% CI, 2.78–12.68) after shoulder/proximal humerus fracture.

With death treated as a competing event, the cumulative incidence of first refracture was 1.67% (95% CI, 1.30–2.04) at 1 year, 4.76% (95% CI, 4.07–5.45) at 3 years, and 8.41% (95% CI, 7.30–9.51) at 5 years (Fig. 2C; Table 2). Across the observed follow-up period, the absolute burden of mortality exceeded that of first refracture. Fracture-specific cumulative incidence functions are shown in Supplementary Fig. S4.

Prognostic associations with mortality and refracture

After multivariable adjustment, female sex was associated with lower all-cause mortality than male sex (HR, 0.64; 95% CI, 0.54–0.76) (Fig. 3A; Table 3). Higher ASA class and greater comorbidity burden were associated with higher mortality, with an HR of 1.57 (95% CI, 1.31–1.90) for ASA III–IV versus I–II and 1.31 (95% CI, 1.19–1.44) per one-point increase in the source-provided CCI.

Table 3
Adjusted prognostic associations

Section	Factor	Mortality HR	Refracture cause-specific HR	Refracture Fine–Gray sHR
A. All-cause mortality	Age: restricted cubic spline (54, 68, 85 years)	See Fig. 3B; reference age 68 years	—	—
A. All-cause mortality	Female vs male	0.64 (0.54–0.76)	—	—
A. All-cause mortality	Lumbar spine/pelvis vs hip/femur	0.78 (0.62–0.98)	—	—
A. All-cause mortality	Thoracic spine/rib vs hip/femur	0.65 (0.48–0.88)	—	—
A. All-cause mortality	Forearm/wrist vs hip/femur	0.47 (0.28–0.80)	—	—
A. All-cause mortality	Shoulder/proximal humerus vs hip/femur	0.36 (0.19–0.71)	—	—
A. All-cause mortality	ASA III-IV vs I-II	1.57 (1.31–1.90)	—	—
A. All-cause mortality	CCI, per point	1.31 (1.19–1.44)	—	—
B. First refracture	Age, per 10 years	—	1.45 (1.26–1.67)	1.36 (1.18–1.57)
B. First refracture	Female vs male	—	1.47 (1.09–1.98)	1.54 (1.14–2.08)
B. First refracture	Lumbar spine/pelvis vs hip/femur	—	1.61 (1.15–2.24)	1.69 (1.17–2.44)
B. First refracture	Thoracic spine/rib vs hip/femur	—	1.61 (1.11–2.34)	1.73 (1.17–2.55)
B. First refracture	Forearm/wrist vs hip/femur	—	1.26 (0.79–2.02)	1.32 (0.81–2.15)
B. First refracture	Shoulder/proximal humerus vs hip/femur	—	0.99 (0.50–1.93)	1.07 (0.54–2.14)
B. First refracture	CCI, per point	—	1.25 (1.05–1.50)	1.20 (0.99–1.44)

Selected core clinical associations from the unchanged fully adjusted models. BMI, haemoglobin, albumin, log2 creatinine, and admission year remain in the fitted models; their complete results are reported in Tables S2 and S3. Hip/femur fracture is the reference. CCI does not include age points.

Compared with hip/femur fracture, mortality was lower after lumbar spine/pelvis fracture (HR, 0.78; 95% CI, 0.62–0.98), thoracic spine/rib fracture (HR, 0.65; 95% CI, 0.48–0.88), forearm/wrist fracture (HR, 0.47; 95% CI, 0.28–0.80), and shoulder/proximal humerus fracture (HR, 0.36; 95% CI, 0.19–0.71). The association between age and mortality was nonlinear (Fig. 3B), with evidence of both an overall association and departure from linearity. Full adjusted estimates are provided in Table S2.

The prognostic pattern for refracture differed from that for mortality (Fig. 3C; Table 3). Each 10-year increase in age was associated with a higher refracture rate in both the cause-specific model (HR, 1.45; 95% CI, 1.26–1.67) and the Fine–Gray model (sHR, 1.36; 95% CI, 1.18–1.57). Female sex, despite being associated with lower mortality, was associated with a higher risk of first refracture (cause-specific HR, 1.47; 95% CI, 1.09–1.98; sHR, 1.54; 95% CI, 1.14–2.08).

A similar contrast was observed across fracture categories. Relative to hip/femur fracture, lumbar spine/pelvis fracture was associated with a higher refracture rate (cause-specific HR, 1.61; 95% CI, 1.15–2.24; sHR, 1.69; 95% CI, 1.17–2.44), as was thoracic spine/rib fracture (cause-specific HR, 1.61; 95% CI, 1.11–2.34; sHR, 1.73; 95% CI, 1.17–2.55), although both categories were associated with lower adjusted mortality. Estimates for forearm/wrist and shoulder/proximal humerus fractures were less precise, with confidence intervals including the null. The source-provided CCI was associated with refracture in the cause-specific analysis (HR, 1.25; 95% CI, 1.05–1.50), whereas the corresponding Fine–Gray estimate was less precise (sHR, 1.20; 95% CI, 0.99–1.44). Complete estimates for all covariates are reported in Table S3.

Descriptive post-fracture disease transitions

Using the common cutoff of March 24, 2024, 252 first refractures and 567 deaths were observed. Among patients without prior refracture, 252 experienced a first refracture and 516 died directly. A further 51 deaths occurred after first refracture, while 201 patients remained alive or were censored after refracture and 4,005 remained alive without either refracture or death at the common cutoff (Fig. 1D; Table S4).

The crude transition rate from survival without refracture to first refracture was 18.0 per 1,000 person-years (95% CI, 15.8–20.3), compared with 36.8 per 1,000 person-years (95% CI, 33.7–40.1) for direct death without prior refracture. Among patients who experienced a first refracture, the subsequent crude mortality rate was 93.9 per 1,000 person-years (95% CI, 69.9–123.5).

Development and internal validation of the 1-year mortality model

Within the development cohort, 201 deaths occurred within 365 days after hospital discharge, while 355 patients were censored alive before 365 days because complete 1-year follow-up was unavailable. The frozen Cox model incorporated nine routinely available clinical inputs: age, sex, fracture category, BMI, ASA class, source-provided CCI, haemoglobin, albumin, and creatinine (Fig. 4A). Full model coefficients,

predictor centres, transformations, and the baseline survival function at 365 days are provided in Table S5.

A nomogram derived directly from the frozen model, without refitting, is presented in Fig. 4B. Predictor-specific contributions are mapped to total points and the corresponding absolute 365-day post-discharge mortality risk. Age retained its restricted cubic-spline specification, and creatinine retained its internal log2 transformation.

In internal validation using 500 patient-level bootstrap samples with re-estimation of the multiple-imputation model within each resample, the optimism-corrected 365-day IPCW time-dependent AUC was 0.860, Harrell's C statistic was 0.857, and the censoring-adjusted Brier score was 0.03695. The optimism-corrected calibration slope was 0.958 and the O/E ratio was 1.008 (Fig. 4C; Table 4). Internal-validation results are reported as point estimates because the replicate-specific corrected distributions reflect variation in estimated optimism rather than full sampling uncertainty (Supplementary Fig. S6; Table S6).

Table 4
Performance of the frozen 1-year mortality model

Metric	Strict internal validation	External validation
AUC	0.860	0.802 (0.709–0.884)
Harrell C	0.857	0.794 (0.705–0.874)
Brier score	0.03695	0.03552 (0.02401–0.04856)
Calibration slope	0.958	0.849 (0.540–1.237)
O/E	1.008	1.006 (0.667–1.387)

Internal validation values are optimism-corrected point estimates; no ordinary 95% confidence intervals are reported. External-validation values retain bootstrap 95% confidence intervals.

Outcome-informed imputation sensitivity analysis

In the development cohort, BMI was missing in 755 patients (15.8%), haemoglobin in 91 (1.9%), albumin in 155 (3.2%), and creatinine in 59 (1.2%). The primary multiple-imputation model included 17 baseline variables (Table S6).

Adding the 365-day mortality indicator and standardized Nelson–Aalen cumulative hazard to the imputation model resulted in only minimal changes to the fitted prediction model. The direction of all regression coefficients was preserved, and external discrimination and calibration remained essentially unchanged. The external AUC changed from 0.802 to 0.801, the calibration slope remained 0.849, and the O/E ratio changed from 1.006 to 1.011 (Table S6).

External validation and risk stratification

When applied without refitting to the independent hospital cohort, the frozen model retained good discrimination. Because 365-day mortality status was complete for all 695 external-validation patients, the external AUC was calculated from the binary 365-day outcome and was 0.802 (95% CI, 0.709–0.884). Harrell's C statistic was 0.794 (95% CI, 0.705–0.874) (Fig. 4C; Table 4), and the external 365-day Brier score was 0.03552 (95% CI, 0.02401–0.04856).

Overall calibration was close, with a calibration slope of 0.849 (95% CI, 0.540–1.237) and an O/E ratio of 1.006 (95% CI, 0.667–1.387) (Fig. 4D). Linear-predictor distributions were broadly similar between the development and external cohorts, although the external distribution was modestly narrower. The linear-predictor SD was 1.794 in the development cohort and 1.671 in the external cohort, corresponding to an external-to-development SD ratio of 0.931 (95% CI, 0.883–0.978) and an LP standardized mean difference of 0.097 (Table S7).

Observed mortality increased across quintiles of predicted risk (Fig. 4E). Mortality was 0.72% (1/139) in the lowest-risk quintile and 14.39% (20/139) in the highest-risk quintile, compared with corresponding mean predicted risks of 0.15% and 13.49%, respectively. Overall, 20 of the 28 external deaths (71.4%) occurred in the highest predicted-risk quintile.

Model updating and exploratory clinical utility

Updating the frozen model did not produce a stable improvement in external performance (Table S8). Baseline-only recalibration yielded an estimated calibration intercept of − 0.001 (95% CI, − 0.436 to 0.343), with no change in discrimination. Updating both the calibration intercept and slope produced an intercept of − 0.371 (95% CI, − 1.407 to 0.508) and a slope of 0.849 (95% CI, 0.540–1.237), without a stable improvement in Brier performance. The unchanged frozen model was therefore retained as the primary external-validation model.

In exploratory decision-curve analysis, 10 of 40 evaluated thresholds had bootstrap intervals for improvement over the better default strategy that excluded zero (Supplementary Fig. S7).

Discussion

In this retrospective prognostic study, long-term mortality represented a greater absolute burden than first refracture among patients hospitalized with osteoporotic fractures. Five-year all-cause mortality was 17.6%, compared with a 5-year competing-risk cumulative incidence of first refracture of 8.4%. Prognosis varied substantially across fracture categories and patient characteristics. Hip/femur fracture was associated with the greatest mortality burden, whereas several non-hip fracture groups showed lower mortality but higher refracture risk. Female sex showed a similar divergence, with lower mortality but higher refracture risk. In parallel, a parsimonious nine-input Cox model retained good discrimination and close overall calibration for 1-year post-discharge mortality when applied without refitting to an independent hospital cohort.

The observed mortality burden is consistent with previous population-based studies showing that excess mortality after osteoporotic fracture extends beyond hip fracture [1–4]. Hip/femur fracture was associated with the highest long-term mortality in our cohort, whereas lumbar spine/pelvis and thoracic spine/rib fractures showed lower adjusted mortality but higher refracture hazards. Previous studies have likewise reported substantial mortality after pelvic and proximal humeral fractures [37–40], while distal radius fracture generally carries lower short-term mortality but remains an important marker of subsequent fracture risk [41]. Together, these findings highlight the prognostic heterogeneity of osteoporotic fractures and support interpretation according to fracture category rather than assuming a uniform post-fracture course.

Sex showed a similarly divergent prognostic pattern. Women had lower adjusted mortality than men but a higher risk of first refracture, consistent with previous fragility-fracture studies [1–3]. Differences in frailty, comorbidity burden, skeletal health, falls, and competing mortality may contribute to this pattern, although these mechanisms were not directly evaluated. The contrasting associations nevertheless reinforce that mortality and refracture represent distinct dimensions of post-fracture prognosis and are best considered separately.

Competing mortality was particularly relevant when estimating refracture risk. Older patients, especially those with hip/femur fractures, may die before a subsequent fracture occurs. Treating these deaths as ordinary censoring can overestimate the cumulative probability of refracture. Cause-specific Cox and Fine–Gray models therefore provided complementary perspectives: the former estimated refracture hazard among patients who remained alive and refracture-free, whereas the latter characterized cumulative refracture incidence in the presence of competing death [27, 28]. The broadly consistent direction of associations across the two approaches supports the overall interpretation of the refracture findings.

The descriptive transition analysis provided additional context for the relationship between refracture and death. Direct death from the refracture-free state occurred more frequently than first refracture, while a further group of patients died after experiencing a refracture. This pattern is consistent with previous work describing fracture, refracture, and death as interconnected adverse outcomes [3].

The prediction model complemented the long-term outcome analyses by estimating 1-year post-discharge mortality using routinely available clinical information. Most established mortality tools have been developed in surgical hip-fracture populations and primarily target short-term postoperative outcomes [20, 21]. In contrast, the present model covered a broader osteoporotic-fracture population and was evaluated using bootstrap internal validation followed by independent external validation without model refitting.

External discrimination remained good, with an AUC of 0.802, and overall calibration was close, with an O/E ratio near 1. The calibration slope was below 1 but compatible with 1 within its confidence interval. The external linear-predictor distribution was modestly narrower than that of the development cohort,

indicating somewhat less variation in predicted risk. Recalibration did not materially improve external performance, and the unchanged frozen model was therefore retained.

The outcome-informed multiple-imputation sensitivity analysis further supported the stability of the prediction findings. Adding the 365-day mortality indicator and standardized Nelson–Aalen cumulative hazard to the imputation model resulted in only minimal changes in regression coefficients, individual predictions, and external performance [34]. The principal findings were therefore consistent across the two imputation strategies.

Decision-curve analysis suggested potential net benefit across part of the evaluated threshold range, although no intervention threshold was prespecified. The model may therefore provide a reproducible framework for post-fracture mortality risk stratification and for further evaluation within clinical care pathways. Future studies can assess whether integrating mortality-risk stratification with fracture liaison services or other secondary-prevention programmes improves the targeting of follow-up, multidisciplinary assessment, and post-fracture care [42–44].

Strengths and limitations

This study has several strengths. Mortality and refracture were evaluated within the same large osteoporotic-fracture cohort, allowing direct comparison of two clinically important and competing outcomes. Refracture was analysed using competing-risk methods and complemented by descriptive transition analyses. The prediction model incorporated a limited number of routinely available variables, underwent bootstrap internal validation with re-estimation of the imputation model, and was subsequently evaluated without refitting in an independent hospital cohort.

Several limitations should be considered. Both the development and external validation cohorts were retrospective, and residual confounding, misclassification, and incomplete capture of clinical information remain possible. Refractures treated outside the healthcare systems covered by the source regional platform may not have been captured. The public dataset also lacked precise within-hospital measurement times for several predictors and did not consistently include potentially relevant factors such as frailty, functional status, falls, socioeconomic characteristics, detailed bone mineral density measurements, or longitudinal treatment adherence. The external cohort included 28 deaths within 365 days, which reduced the precision of some validation estimates, particularly calibration. Both cohorts were derived from Chinese healthcare settings, and validation in other populations and healthcare systems would further establish generalizability. Finally, the model estimates risk using information available during the index hospitalization and does not incorporate subsequent changes in clinical status, treatment, or recurrent fracture.

Clinical implications

Post-fracture prognosis is better characterized by considering mortality and refracture together while recognizing that they follow different prognostic patterns. Hip/femur fracture identified a group with particularly high long-term mortality, whereas some non-hip fracture groups had lower mortality but appreciable subsequent fracture risk. These differences may help inform the intensity and focus of post-fracture follow-up.

The proposed model provides a reproducible approach to 1-year post-discharge mortality risk stratification using routinely available clinical information. Its application may help identify patients at higher post-discharge mortality risk and provide a basis for evaluating targeted follow-up or multidisciplinary post-fracture care. Larger and more diverse external validation studies, together with prospective evaluation of risk-informed care pathways, would help define its role alongside established secondary-prevention strategies.

Conclusion

Among patients hospitalized with osteoporotic fractures, long-term mortality exceeded the cumulative incidence of first refracture and varied substantially across fracture categories and patient characteristics. Mortality and refracture showed distinct prognostic patterns, underscoring the importance of accounting for competing death when evaluating post-fracture outcomes. A parsimonious nine-input Cox model retained good discrimination and close overall calibration for 1-year post-discharge mortality in an independent hospital cohort. These findings provide a basis for broader validation and further evaluation of risk-stratified post-fracture care.

Abbreviations

ASA, American Society of Anesthesiologists; AUC, area under the receiver operating characteristic curve; BMI, body mass index; CCI, Charlson Comorbidity Index; CIF, cumulative incidence function; DXA, dual-energy X-ray absorptiometry; FLS, fracture liaison service; HR, hazard ratio; IPCW, inverse probability of censoring weighting; MI, multiple imputation; O/E, observed-to-expected ratio; OPFRS, Osteoporotic Fracture Registration System; RCS, restricted cubic spline; sHR, subdistribution hazard ratio; SMD, standardized mean difference.

Declarations

Acknowledgements

The authors thank the investigators who established and publicly shared the Osteoporotic Fracture Registration System dataset and the clinical and research staff at Wuhan Integrated Traditional Chinese and Western Medicine Orthopedic Hospital/Affiliated Hospital of Wuhan Sports University for their contributions to the independent external validation cohort.

Author contributions

JX contributed to investigation, data curation, resources, and manuscript review and editing. TL contributed to investigation, resources, project administration, and manuscript review and editing. BH contributed to investigation, data curation, resources, and manuscript review and editing. JM contributed to conceptualization, methodology, supervision, and manuscript review and editing. CX contributed to investigation, data curation, resources, and manuscript review and editing. FX contributed to conceptualization, supervision, resources, project administration, and manuscript review and editing. QL contributed to conceptualization, supervision, resources, project administration, and manuscript review and editing. HH contributed to conceptualization, methodology, formal analysis, data curation, validation, visualization, software, preparation of the original draft, and manuscript review and editing.

JX, TL, and BH contributed equally to this work. All authors read and approved the final manuscript.

Funding

HH was supported by the China Scholarship Council (grant No. 202308420016). The funder had no role in the study design; data acquisition, management, analysis, or interpretation; development or validation of the prediction model; preparation, review, or approval of the manuscript; or the decision to submit the manuscript for publication.

Availability of data and materials

The development dataset analysed in this study is publicly available from Figshare:

A longitudinal clinical and prescription dataset of hypertensive osteoporotic fracture patients.
DOI: 10.6084/m9.figshare.30971476.v1

The public release includes the clinical-variable dataset, medication records, and variable-definition table described in the original data publication.

Individual-level data from the independent external validation cohort are not publicly available because of institutional ethics, patient-privacy, and data-governance requirements. De-identified external-validation data may be available from the corresponding author on reasonable request, subject to approval by the responsible institution and applicable ethics and data-use requirements.

The complete frozen prediction-model specification, including predictor definitions, transformations, regression coefficients, predictor centres, and the 365-day baseline survival function, is provided in the Supplementary Materials to support reproducibility.

Ethics approval and consent to participate

The development cohort was derived from a publicly available, de-identified dataset originating from the Osteoporotic Fracture Registration System at the Affiliated Kunshan Hospital of Jiangsu University, Jiangsu Province, China. The source registry study was approved by the Institutional Review Board of the Affiliated Kunshan Hospital of Jiangsu University (approval No. 2024-03-053-H00-K01). As reported in the original data publication, the requirement for individual informed consent was waived because of the retrospective study design and use of de-identified data.

The independent external validation study was approved by the Ethics Committee of Wuhan Integrated Traditional Chinese and Western Medicine Orthopedic Hospital/Affiliated Hospital of Wuhan Sports University (approval No. 672HREC20260522-L044). The requirement for individual informed consent was waived by the ethics committee because of the retrospective design and use of routinely collected clinical data.

Both study components were conducted in accordance with the Declaration of Helsinki.

Clinical trial number

Not applicable.

Consent for publication

Not applicable.

Competing interests

The authors declare that they have no competing interests.

References

1. Center JR, Nguyen TV, Schneider D, Sambrook PN, Eisman JA. Mortality after all major types of osteoporotic fracture in men and women: an observational study. Lancet. 1999;353(9156):878–82.
2. Johnell O, Kanis JA, Odén A, et al. Mortality after osteoporotic fractures. Osteoporos Int. 2004;15(1):38–42. 10.1007/s00198-003-1490-4.
3. Bliuc D, Nguyen ND, Milch VE, Nguyen TV, Eisman JA, Center JR. Mortality risk associated with low-trauma osteoporotic fracture and subsequent fracture in men and women. JAMA. 2009;301(5):513–21. 10.1001/jama.2009.50.

4. Haentjens P, Magaziner J, Colón-Emeric CS, et al. Meta-analysis: excess mortality after hip fracture among older women and men. Ann Intern Med. 2010;152(6):380–90. 10.7326/0003-4819-152-6-201003160-00008.
5. Kado DM, Browner WS, Palermo L, Nevitt MC, Genant HK, Cummings SR. Vertebral fractures and mortality in older women: a prospective study. Arch Intern Med. 1999;159(11):1215–20. 10.1001/archinte.159.11.1215.
6. Tran TS, Bliuc D, Hansen L, et al. Population-wide impact of non-hip non-vertebral fractures on mortality. J Bone Min Res. 2017;32(9):1802–10.
7. Brown JP, Adachi JD, Schemitsch E, et al. Mortality in older adults following a fragility fracture: real-world retrospective matched-cohort study in Ontario. BMC Musculoskelet Disord. 2021;22:105.
8. Global Burden of Disease. 2019 Fracture Collaborators. Global, regional, and national burden of bone fractures in 204 countries and territories, 1990–2019: a systematic analysis from the Global Burden of Disease Study 2019. Lancet Healthy Longev. 2021;2(9):e580–e592.
9. Borgström F, Karlsson L, Ortsäter G, et al. Fragility fractures in Europe: burden, management and opportunities. Arch Osteoporos. 2020;15:59. 10.1007/s11657-020-0706-y.
10. Sing CW, Lin TC, Bartholomew S, et al. Global epidemiology of hip fractures: secular trends in incidence rate, post-fracture treatment, and all-cause mortality. J Bone Min Res. 2023;38(8):1064–75. 10.1002/jbmr.4821.
11. Johnell O, Kanis JA, Odén A, et al. Fracture risk following an osteoporotic fracture. Osteoporos Int. 2004;15(3):175–9. 10.1007/s00198-003-1514-0.
12. Lindsay R, Silverman SL, Cooper C, et al. Risk of new vertebral fracture in the year following a fracture. JAMA. 2001;285(3):320–3. 10.1001/jama.285.3.320.
13. Johansson H, Siggeirsdóttir K, Harvey NC, et al. Imminent risk of fracture after fracture. Osteoporos Int. 2017;28(3):775–80. 10.1007/s00198-016-3868-0.
14. Banefelt J, Åkesson KE, Spångéus A, et al. Risk of imminent fracture following a previous fracture in a Swedish database study. Osteoporos Int. 2019;30(3):601–9. 10.1007/s00198-019-04852-8.
15. Balasubramanian A, Zhang J, Chen L, et al. Risk of subsequent fracture after prior fracture among older women. Osteoporos Int. 2019;30(1):79–92. 10.1007/s00198-018-4732-1.
16. Bliuc D, Nguyen TV, Eisman JA, Center JR. The impact of nonhip nonvertebral fractures in elderly women and men. J Clin Endocrinol Metab. 2014;99(2):415–23.
17. Praveen AD, Aspelund T, Ferguson SJ, et al. Refracture and mortality risk in the elderly with osteoporotic fractures: the AGES-Reykjavik study. Osteoporos Int. 2024;35:1231–41. 10.1007/s00198-024-07096-3.
18. Tran TS, Bliuc D, Blank RD, Center JR, Nguyen TV. Fracture risk assessment in the presence of competing risk of death. Osteoporos Int. 2024;35:1989–98. 10.1007/s00198-024-07224-z.
19. Bliuc D, Alarkawi D, Nguyen TV, Eisman JA, Center JR. Risk of subsequent fractures and mortality in elderly women and men with fragility fractures with and without osteoporotic bone density: the

Dubbo Osteoporosis Epidemiology Study. J Bone Min Res. 2015;30(4):637–46.

20. Maxwell MJ, Moran CG, Moppett IK. Development and validation of a preoperative scoring system to predict 30 day mortality in patients undergoing hip fracture surgery. Br J Anaesth. 2008;101(4):511–7.
21. Karres J, Heesakkers NA, Ultee JM, Vrouenraets BC. Predicting 30-day mortality following hip fracture surgery: evaluation of six risk prediction models. Injury. 2015;46(2):371–7.
22. Li C, Shi Q, Gong YQ, Zhang T, Lu K. Development and validation of a prognostic nomogram for 3-year all-cause mortality risk among elderly patients undergoing surgery for osteoporotic fractures. Front Med (Lausanne). 2024;11:1284207. 10.3389/fmed.2024.1284207.
23. Van Calster B, McLernon DJ, van Smeden M, Wynants L, Steyerberg EW. Calibration: the Achilles heel of predictive analytics. BMC Med. 2019;17:230. 10.1186/s12916-019-1466-7.
24. Vickers AJ, Elkin EB. Decision curve analysis: a novel method for evaluating prediction models. Med Decis Mak. 2006;26(6):565–74.
25. Li C, Lu K, Su LW, et al. A longitudinal dataset of hypertensive osteoporotic fracture patients: treatments and long-term outcomes. Sci Data. 2026;13:671. 10.1038/s41597-026-07031-7.
26. LeBoff MS, Greenspan SL, Insogna KL, et al. The clinician's guide to prevention and treatment of osteoporosis. Osteoporos Int. 2022;33(10):2049–102. 10.1007/s00198-021-05900-y.
27. Fine JP, Gray RJ. A proportional hazards model for the subdistribution of a competing risk. J Am Stat Assoc. 1999;94(446):496–509.
28. Austin PC, Fine JP. Practical recommendations for reporting Fine–Gray model analyses for competing risk data. Stat Med. 2017;36(27):4391–400.
29. Harrell FE Jr. Regression Modeling Strategies: With Applications to Linear Models, Logistic and Ordinal Regression, and Survival Analysis. 2nd ed. Cham: Springer; 2015.
30. Grambsch PM, Therneau TM. Proportional hazards tests and diagnostics based on weighted residuals. Biometrika. 1994;81(3):515–26.
31. Gray RJ. A class of K-sample tests for comparing the cumulative incidence of a competing risk. Ann Stat. 1988;16(3):1141–54.
32. Harrell FE Jr, Lee KL, Mark DB. Multivariable prognostic models: issues in developing models, evaluating assumptions and adequacy, and measuring and reducing errors. Stat Med. 1996;15(4):361–87.
33. White IR, Royston P, Wood AM. Multiple imputation using chained equations: issues and guidance for practice. Stat Med. 2011;30(4):377–99. 10.1002/sim.4067.
34. White IR, Royston P. Imputing missing covariate values for the Cox model. Stat Med. 2009;28(15):1982–98. 10.1002/sim.3618.
35. von Elm E, Altman DG, Egger M, Pocock SJ, Gøtzsche PC, Vandenbroucke JP, STROBE Initiative. The Strengthening the Reporting of Observational Studies in Epidemiology (STROBE) statement: guidelines for reporting observational studies. Lancet. 2007;370(9596):1453–7.

36. Collins GS, Moons KGM, Dhiman P, et al. TRIPOD + AI statement: updated guidance for reporting clinical prediction models that use regression or machine learning methods. BMJ. 2024;385:e078378. 10.1136/bmj-2023-078378.
37. Prieto-Alhambra D, Avilés FF, Judge A, et al. Burden of pelvis fracture: a population-based study of incidence, hospitalisation and mortality. Osteoporos Int. 2012;23:2797–803.
38. Taillandier J, Langue F, Alemanni M, Taillandier-Heriche E. Mortality and functional outcomes of pelvic insufficiency fractures in older patients. Joint Bone Spine. 2003;70(4):287–9. 10.1016/S1297-319X(03)00015-0.
39. Sumrein BO, Berg HE, Launonen AP, et al. Mortality following proximal humerus fracture—a nationwide register study of 147,692 fracture patients in Sweden. Osteoporos Int. 2023;34(2):349–56. 10.1007/s00198-022-06612-7.
40. Walter N, Szymski D, Kurtz SM, et al. Proximal humerus fractures—epidemiology, comparison of mortality rates after surgical versus non-surgical treatment, and analysis of risk factors based on Medicare registry data. Bone Joint Res. 2023;12(2):103–12. 10.1302/2046-3758.122.BJR-2022-0275.R1.
41. Bynum JPW, Bell JE, Cantu RV, et al. Second fractures among older adults in the year following hip, shoulder, or wrist fracture. Osteoporos Int. 2016;27:2207–15. 10.1007/s00198-016-3542-6.
42. Wu CH, Chen CH, Chen PH, et al. Identifying characteristics of an effective fracture liaison service: systematic literature review. Osteoporos Int. 2018;29(5):1023–47. 10.1007/s00198-017-4370-z.
43. Danazumi MS, Lightbody N, Dermody G. Effectiveness of fracture liaison service in reducing the risk of secondary fragility fractures in adults aged 50 and older: a systematic review and meta-analysis. Osteoporos Int. 2024;35:1133–51. 10.1007/s00198-024-07052-1.
44. Andreasen C, Dahl C, Frihagen F, et al. Fracture liaison service (FLS) is associated with lower subsequent fragility fracture risk and mortality: NoFRACT (the Norwegian capture the fracture initiative). Osteoporos Int. 2025;36(3):501–12. 10.1007/s00198-024-07376-y.

Figures

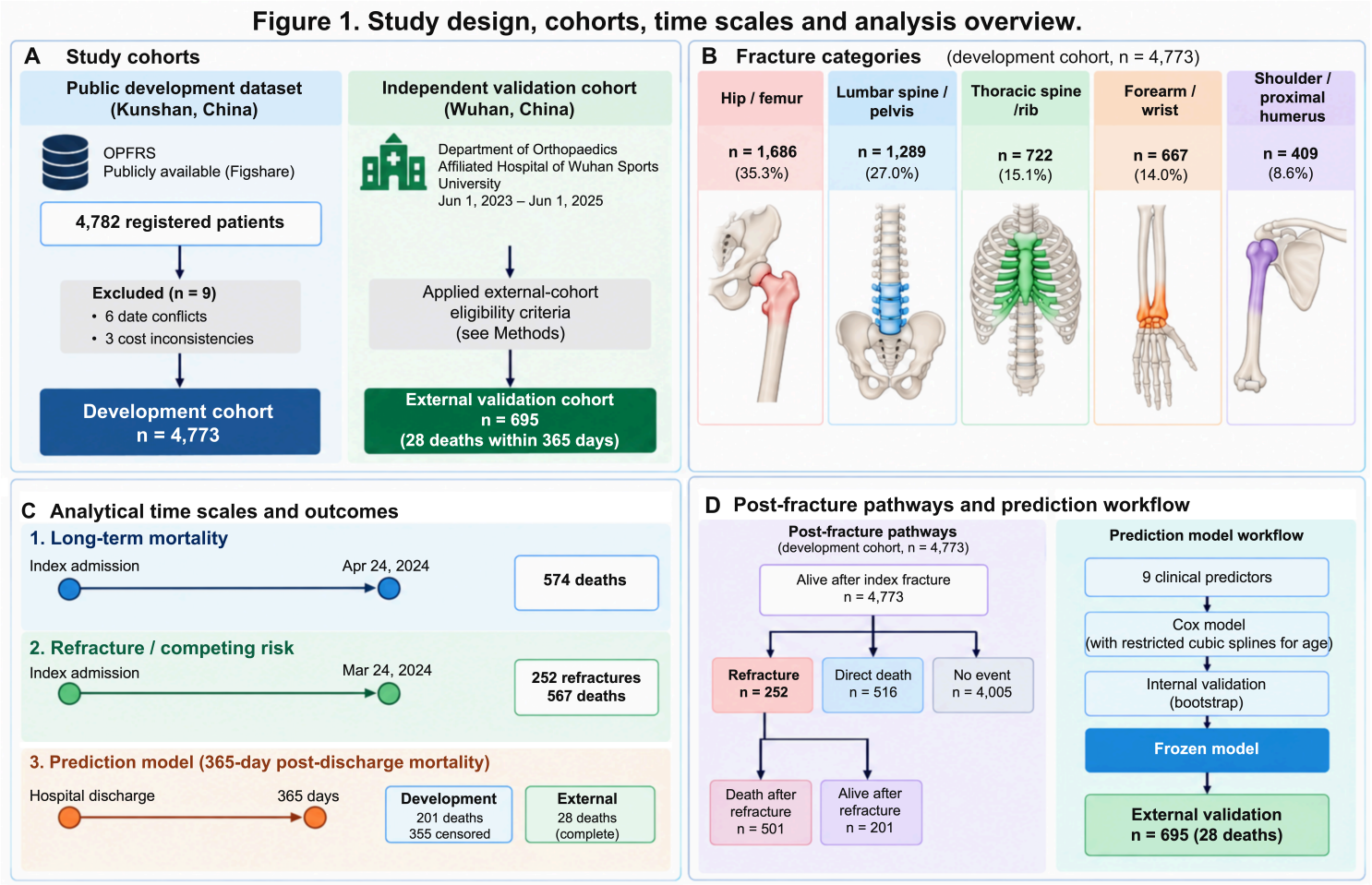


Figure 1

Study design, cohort construction, analytical time scales, and post-fracture pathways.

A, Construction of the public development cohort and the independent hospital-based external validation cohort. The development cohort was reconstructed from the publicly available OPFRS dataset. Of 4,782 registered patients, six records with irreconcilable date conflicts and three with inconsistent total-cost information were excluded, leaving 4,773 patients. The external validation cohort included 695 patients treated between June 1, 2023 and June 1, 2025, of whom 28 died within 365 days after discharge.

B, Distribution of the five index-fracture categories in the development cohort.

C, Outcome-specific analytical time scales. Long-term mortality was assessed from index admission through April 24, 2024. Refracture and descriptive transition analyses used index admission as time zero and March 24, 2024 as the common administrative cutoff, with death treated as a competing event for first refracture. The prediction model targeted all-cause mortality within 365 days after hospital discharge.

D, Descriptive post-fracture pathways and prediction-model workflow. Post-fracture transitions included first refracture, direct death without prior refracture, and death after refracture. The nine-input Cox model was internally validated by bootstrap resampling, frozen, and then applied without refitting to the independent external validation cohort.

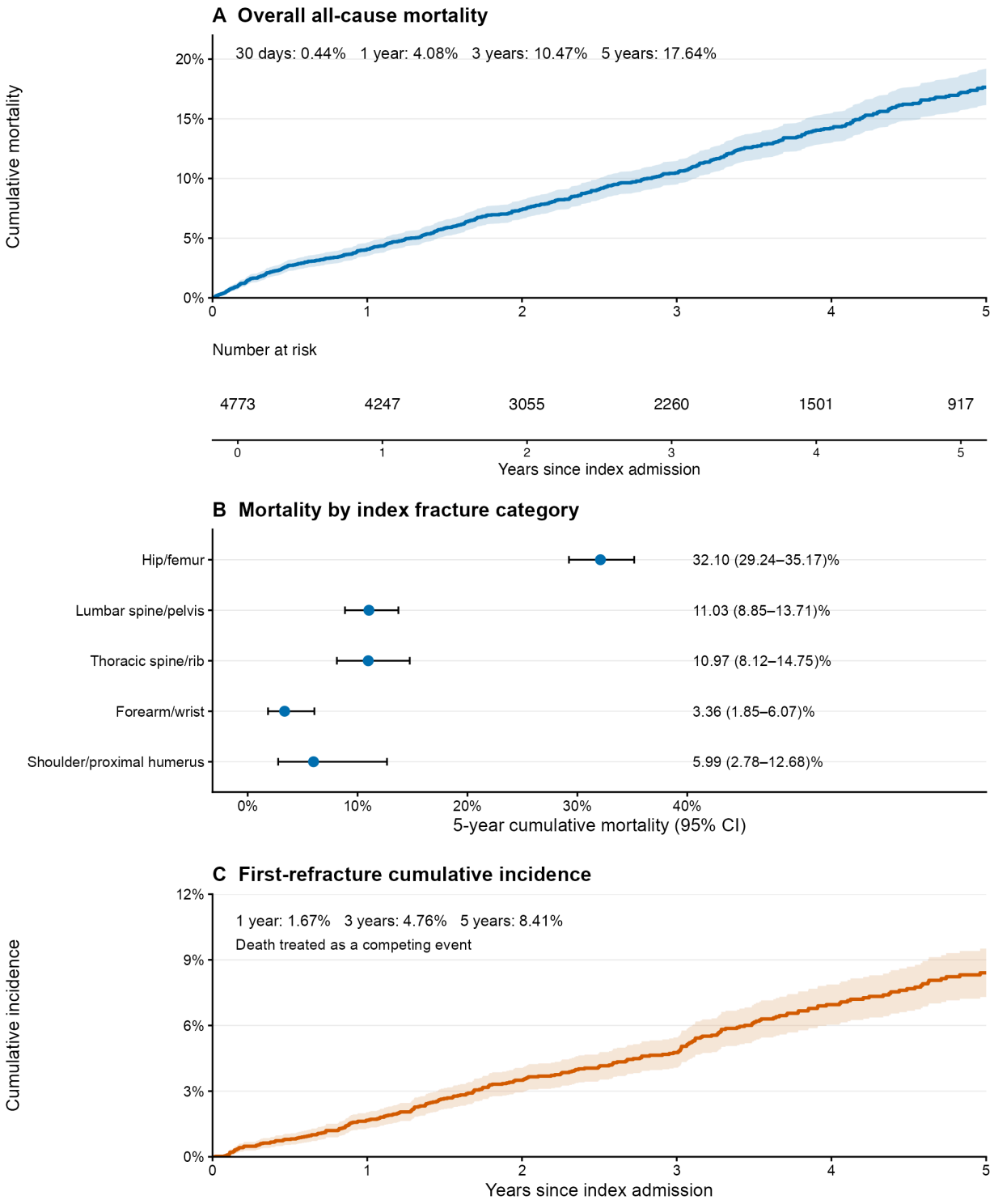


Figure 2

Absolute risks of mortality and first refracture after osteoporotic fracture.

A, Kaplan–Meier cumulative all-cause mortality from index admission, with 95% confidence bands and numbers at risk shown at yearly intervals.

B, Five-year cumulative mortality across the five index-fracture categories. Points represent risk estimates and horizontal bars 95% confidence intervals.

C, Cumulative incidence of first refracture from index admission, with death treated as a competing event. Shaded areas represent 95% confidence intervals.

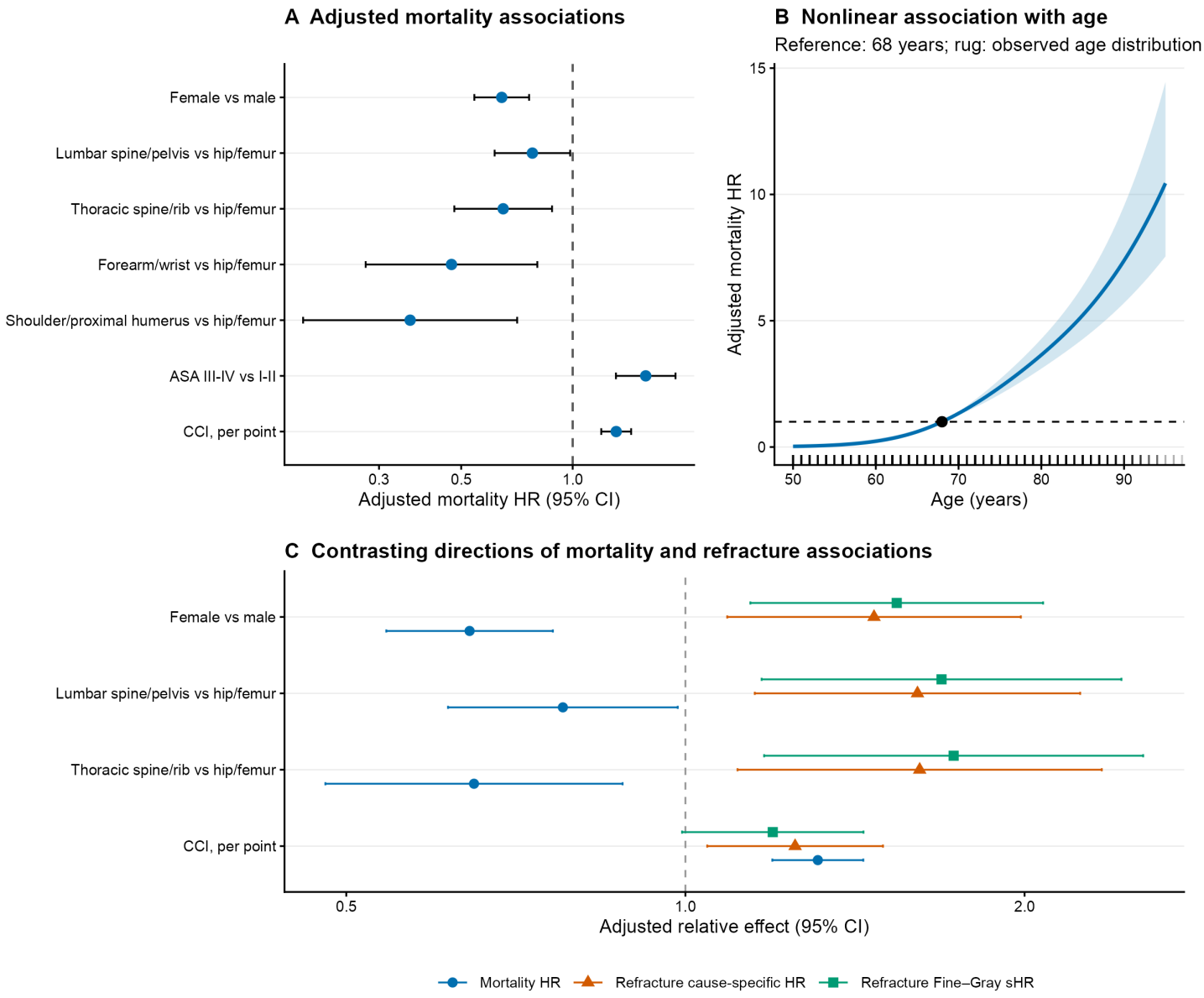


Figure 3

Divergent prognostic associations with mortality and first refracture after osteoporotic fracture.
A, Selected adjusted hazard ratios for all-cause mortality. Hip/femur fracture and male sex served as reference categories; the dashed vertical line denotes HR = 1.
B, Nonlinear association between age and adjusted mortality estimated using restricted cubic splines, with 68 years as the reference. Shading represents the 95% confidence interval, and the rug indicates the observed age distribution.
C, Comparison of adjusted associations for mortality, cause-specific refracture hazard, and Fine–Gray

subdistribution hazard across selected shared clinical factors. Points represent effect estimates and horizontal bars 95% confidence intervals.

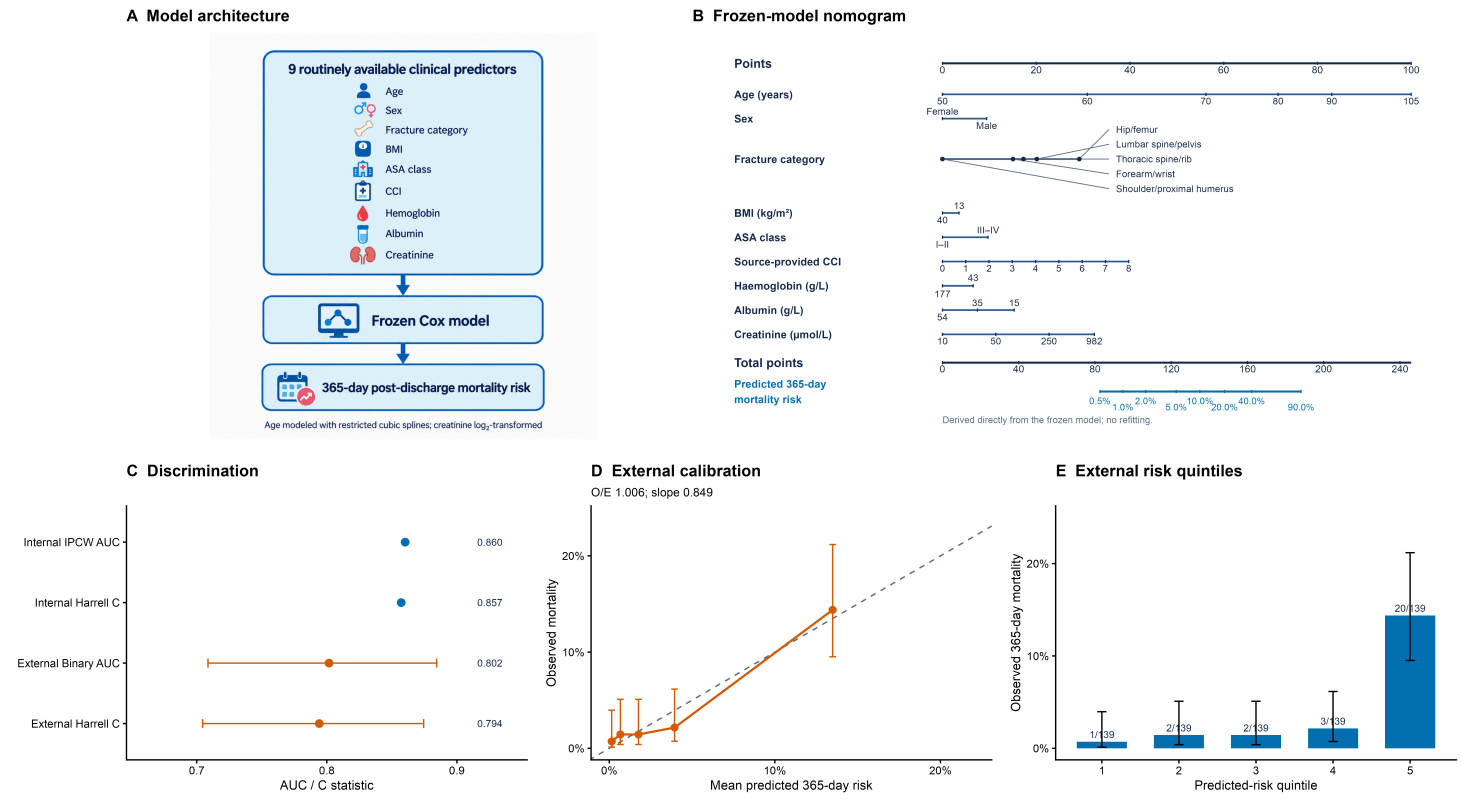


Figure 4

Development and external validation of the frozen 365-day post-discharge mortality model.
A, Architecture of the nine-input Cox model incorporating age, sex, fracture category, BMI, ASA class, source-provided CCI, haemoglobin, albumin, and creatinine. Age was modelled using restricted cubic splines and creatinine was log2-transformed.
B, Nomogram derived directly from the frozen model without refitting, mapping predictor-specific contributions to total points and absolute 365-day mortality risk.
C, Model discrimination in the development and external validation cohorts. Development performance is shown using the 365-day IPCW time-dependent AUC and Harrell's C statistic; external performance is shown using the binary 365-day AUC and Harrell's C statistic.
D, External calibration comparing observed and predicted 365-day mortality; the dashed line indicates perfect calibration.
E, Observed 365-day mortality across quintiles of predicted risk in the external validation cohort. Risk quintiles were used descriptively and were not intended to define clinical intervention thresholds.

Supplementary Files

This is a list of supplementary files associated with this preprint. Click to download.

- Supplementaryfiguresandtables.docx